

## Preparation and characterization of fibrous NiO particles by thermal decomposition of nickelous complex precursors<sup>①</sup>

ZHANG Chuan-fu(张传福), ZHAN Jing(湛菁), WU Jian-hui(邬建辉), LI Chang-jun(黎昌俊)  
(School of Metallurgical Science and Engineering, Central South University, Changsha 410083, China)

**Abstract:** The influences of pyrolytic conditions, including temperature, time, the flow rate of air, and the heating rate, on the morphology, average size and specific surface area of the NiO particles were investigated, and the composition and morphologies of the products were characterized by using of XRD, SEM and BET. It is found that fibrous NiO particles were produced under the optimal conditions. A suitable range of pH for preparing dispersive precursors was chosen according to analysis of zeta potential. Based on the observations of NiO precursors growth and SEM morphology of the precursor, the oriented attachment was proposed for the well aligned growth of the NiO precursor fibres. The final product NiO inherits the morphology of the precursor.

**Key words:** pyrolysis; nickelous complex precursors; NiO fibres; growth mechanism

**CLC number:** O 641.1

**Document code:** A

### 1 INTRODUCTION

In recent years, quasi one-dimensional(1-D) materials with nanostructures (nanowires or fibres) have stimulated considerable interest for scientists because of their importance in mesoscopic physics and potential applications. These nanostructures are expected to have remarkable optical, electrical, and mechanical properties which may get applications in probe microscopy and nanoelectronics<sup>[1, 2]</sup>. In order to obtain one-dimensional structural materials, various preparation methods have been developed including arc discharge, laser ablation, template, solution and other methods<sup>[3-10]</sup>. However, most of the reported experimental techniques for the synthesis of one-dimensional materials are still limited in laboratory scale due to some unresolved problems such as special conditions, the complexity or the high cost. Exploration of novel methods for large-scale synthesis of one-dimensional nanostructure is a challenging research area. As a kind of functional material, nickel oxide(NiO) has received considerable attentions over the last few years because of many applications such as catalysis, electrochromic films, fuel cell electrodes, gas sensors<sup>[11]</sup>. Its importance is manifested in many patents that have been issued for its synthesis. At present the approaches available for NiO powder production include carbonyl method, laser chemical method, pyrolysis by microwave, sol-gel method, pyrolysis by ultrasonic, chemical precipitation etc<sup>[12]</sup>. Most of these

methods have been used to synthesize NiO spherical particles or films, few attempts have been made to prepare NiO fibres. The purpose of this study is to explore the feasibility to synthesize NiO fibres via chemical reaction between  $\text{NiCl}_2 \cdot 6\text{H}_2\text{O}$  and  $(\text{NH}_4)_2\text{C}_2\text{O}_4$  in the presence of surfactant PVP. This method requires neither complex apparatus and sophisticated techniques, nor metal catalysts or templates as usually needed in other methods.

### 2 EXPERIMENTAL

The reagents used in this study, including  $\text{NiCl}_2 \cdot 6\text{H}_2\text{O}$ ,  $\text{NH}_3 \cdot \text{H}_2\text{O}$ ,  $\text{C}_2\text{H}_5\text{OH}$ ,  $\text{CH}_3\text{COCH}_3$ ,  $(\text{NH}_4)_2\text{C}_2\text{O}_4$ , surfactant PVP, were all of analytical purity and used without further purification. The nickelous complex precursor precipitating were carried out in the following procedures. 100 mL  $(\text{NH}_4)_2\text{C}_2\text{O}_4$  (0.6 - 0.8 mol/L) solution was dripped in 100 mL  $\text{Ni}^{2+}$  solution (0.6 - 0.8 mol/L) with SONO-TEK modeled ultrasonic sprayer at a rate of 5 mL/min. During the precipitation reaction, the suspension was kept at constant temperature, in constant pH value and in constant stirring. The suspension was kept stirring for 1h after the reagent addition. Finally, nickelous complex precursors were washed with distilled water and alcohol for several times to remove the possible adsorbed ions, and then dried in vacuum box. The dried precursors were heated in a porcelain crucible that was placed in the middle of an alumina tube with

① **Foundation item:** Project(1998053306) supported by the Doctorate Fund of Education Ministry of China

**Received date:** 2003 - 07 - 29; **Accepted date:** 2004 - 03 - 16

**Correspondence:** ZHAN Jing, PhD; Tel: + 86-731-8836037; E-mail: zhanjing2001@hotmail.com

a horizontal tube electric furnace at 673 ~ 873 K for 1 h. The final product of fibrous NiO were obtained.

The purity and crystallinity of the as-synthesized fibrous NiO were examined by using powder X-ray diffraction (D/max-r A10 Type, Japan). The morphology of the fibres was observed by scanning electron microscope. The zeta potential of the particles was detected to choose a suitable range of pH for disperse precursors. The specific surface area of the decomposed product was measured with ASAP2010 instrument (Micromeritics Company, USA).

### 3 RESULTS AND DISCUSSION

#### 3.1 Inhibition aggregation of precursors

There are several main methods to prevent aggregation of precipitation in solution including controlling precipitation condition, adding dispersant and choosing suitable pH range for disperse particles according to zeta potential. The effect of preparation conditions on morphology of precursor particles were reported in detail in another paper<sup>[12]</sup>. Here, we discuss the mechanism of inhibition aggregation with the respect to zeta potential and surfactant.

It is well-known that the electric double layers of charged particles exert repulsive force against each other which is a function of zeta potential. Accordingly, precipitation from a homogeneous solution is normally carried out in a range away from the point of zero charge. Fig. 1 shows that the pH value for the isoelectric point of the precursors is 2.5. The higher the pH is, the lower the zeta potential value will be. With the increase of solution pH from 8 ~ 10, the zeta potential decreases sharply and becomes negative, so there will be electrostatic repulsion between the dispersant and the particles surface. A moderate alkaline environment (pH < 10) is expected for dispersing precipitation particles, which is in agreement with the moderate alkaline condition for  $\text{NiCl}_2 \cdot (\text{NH}_4)_2\text{C}_2\text{O}_4 \cdot \text{NH}_3$  system in which the solution pH should be 8 ~ 10 throughout the precipitation process.

To stabilize the lyophobic colloidal particles, one of the most effective ways is to use protective agents, including lyophilic polymers, surfactants and complexing agent, which are adsorbed on the particles. It is believed that stabilization occurs mainly through a repulsive force due to the coulomb repulsion and/or the osmotic pressure and the steric hindrance at the overlapped regions of the adsorptive layers of the individual particles<sup>[13]</sup>. The surfactant PVP is favorable to form fine, disperse particles and make a "shell" surrounding the particles to prevent them aggregating to larger particles during the precipitation. From the above analysis, the high dispersion of NiO precursor fibres were obtained by controlling the solution with a pH higher than 8.0 and adding dispersant. The mor-

phologies of precursors are shown as Fig. 2.

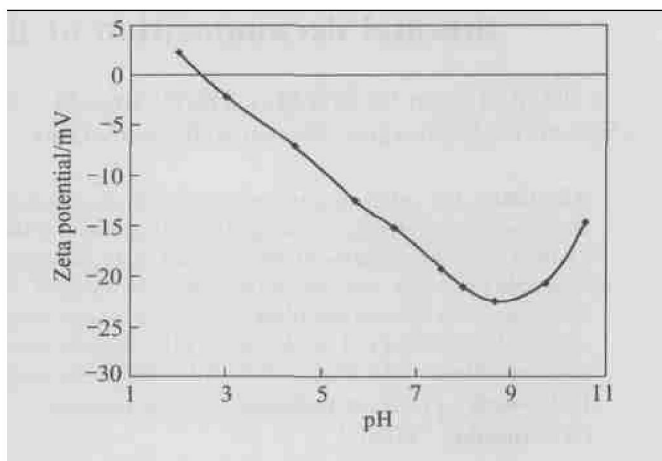


Fig. 1 Zeta potentials of nickelous complex precursor with PVP

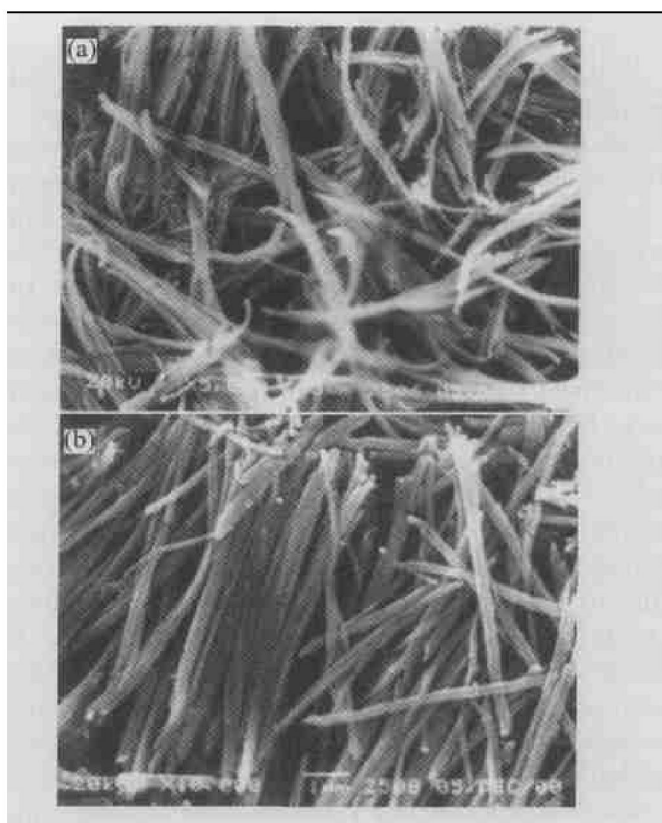


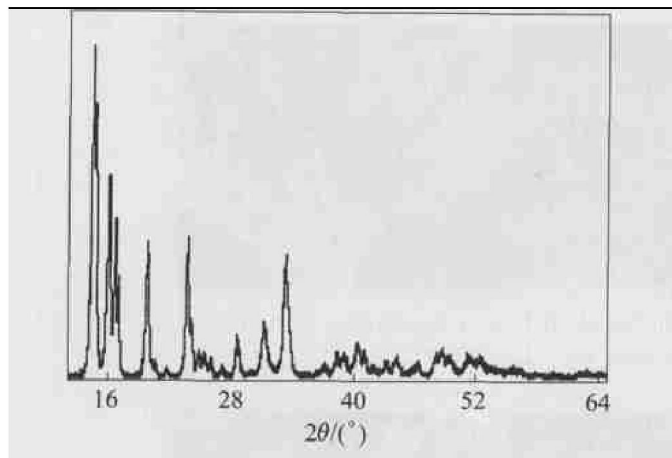
Fig. 2 SEM morphologies of nickelous complex precursors  
(a) —pH= 8.2; (b) —pH= 8.4

Fig. 3 illustrates the X-ray diffraction pattern of the precursor. It can be found that the precursor is crystal structure and there are no  $\text{NiC}_2\text{O}_4 \cdot 2\text{H}_2\text{O}$  peaks, which suggests that the precursor is nickelous complex precipitation instead of pure  $\text{NiC}_2\text{O}_4 \cdot 2\text{H}_2\text{O}$  particles

#### 3.2 Effect of different pyrolysis conditions

##### 3.2.1 Effect of decomposition temperature

The morphology of the NiO particles is depen-



**Fig. 3** XRD pattern of precursor particles

dent on the temperature of pyrolysis. In general, the lower the temperature is, the smaller the particles will be. When the samples are decomposed at 400, 500, 550, 600 °C, the corresponding products are grey, grey-black, light-green and light green. The X-ray diffraction results show that the grey-black product is the mixture of Ni and NiO. This suggests that the mixed Ni and NiO product is produced at the temperature below 600 °C (see Fig. 4). The pure NiO may be obtained at the temperature higher than 600 °C. However, even at higher temperature, the activity of NiO is relatively low, and the aggregation of the particles is serious due to sintering. Fig. 5 shows the SEM morphologies of the NiO particles obtained at temperature from 600 °C to 700 °C. The temperature has less effect on the morphology of the product and the final particles remain fibrous morphology as the same as in precursor.

### 3.2.2 Effect of decomposition time

Fig. 6 illustrates the SEM morphologies of NiO particles obtained with different pyrolysis times. 30 – 60 min is enough for decomposition of the precursor. If it is conducted under shorter time, the decomposition may be incomplete though the produced powder is active with less density. Whereas extending the time for decomposition, the aggregation among the particles becomes serious

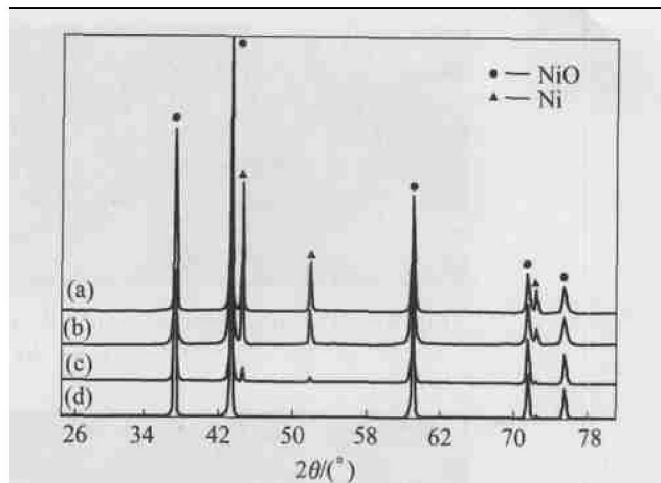


**Fig. 4** XRD patterns of products from precursor decomposed at various temperatures  
(a) –400 °C; (b) –500 °C; (c) –550 °C; (d) –600 °C

and the particles are inactive. So the suitable time for the decomposition is 30 – 60 min.

### 3.2.3 Effect of air flow

The effect of air flow on the morphology of NiO particles is shown in Fig. 7. It is clear that the air flow exerts the influence on both morphology and particle size of the product. In low air flow, the gas generated from the decomposition diffuses slowly and hinders the pyrolysis process. Increasing the air flow is useful for the decomposition. However, if the air flow is too large, it may cause powder emission.

### 3.2.4 Effect of heating method

The heating method has obvious effect on the specific surface area of the product. When the precursor particles are heated together with furnace, the NiO has fine dispersion and satisfactory morphology. However, if the precursor is directly put into the furnace at high temperature and decomposed, the NiO particles are hard and difficult to be broken. By measurement of BET, the specific surface area of the former is larger than 5.944 m<sup>2</sup>/g while that of the later is less than 1 m<sup>2</sup>/g. This is because there are lots of gas emissions in the process of pyrolysis. In the former case, the precursor releases the ammonia first, then water,

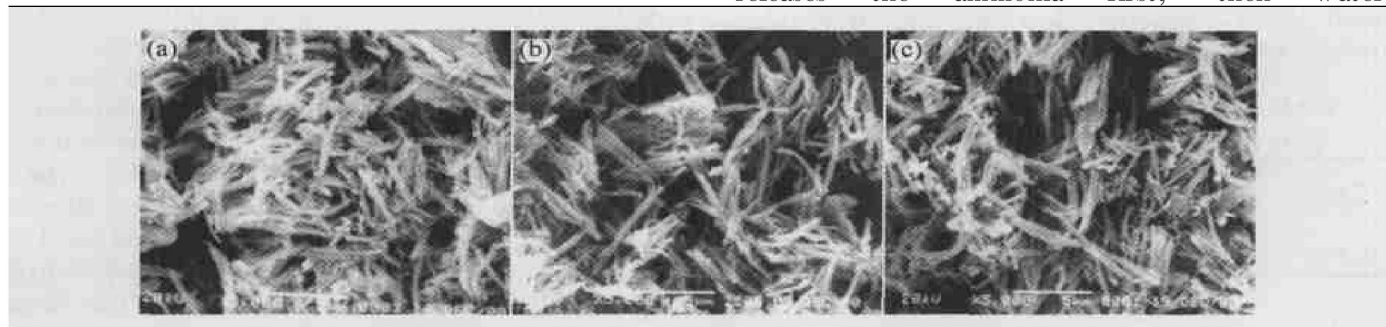


**Fig. 5** SEM morphologies of NiO particles obtained at different pyrolytic temperatures  
(a) –600 °C; (b) –650 °C; (c) –700 °C

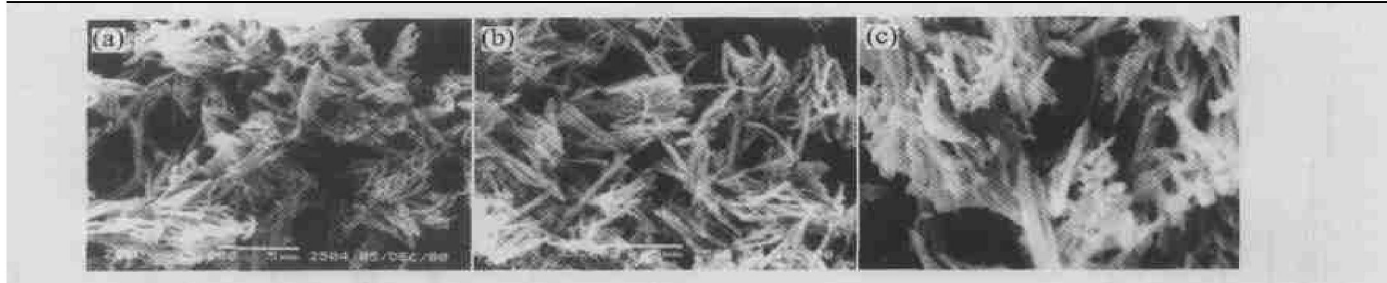


**Fig. 6** SEM morphologies of NiO particles at different decomposition times  
(a) -30 min; (b) -60 min; (c) -120 min

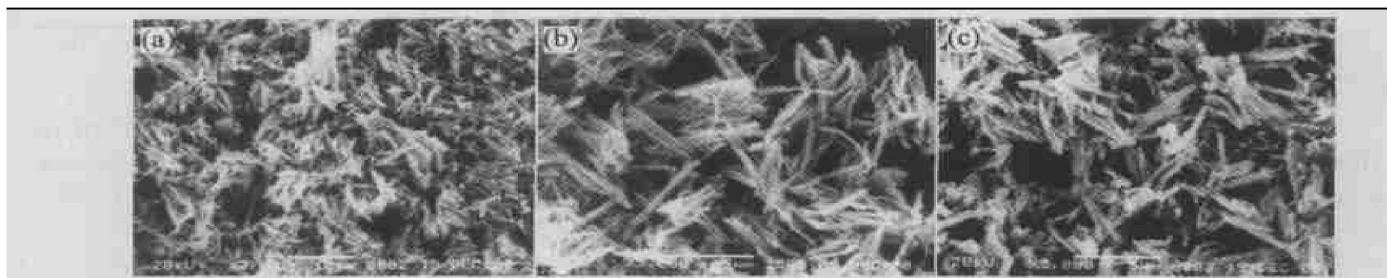


**Fig. 7** SEM morphologies of NiO particles at different air flows  
(a)  $-0.08 \text{ dm}^3/\text{min}$ ; (b)  $-0.124 \text{ dm}^3/\text{min}$ ; (c)  $-0.152 \text{ dm}^3/\text{min}$

and last pyrolysis. By this way, the product is loose as the volume does not change obviously before and after pyrolysis. The morphology of the final particles inherits to the precursors.

### 3.3 Characterization of fibrous NiO fibres

The purity and crystallinity of the as-synthesized fibrous NiO were examined by using powder X-ray diffraction (XRD). Fig. 8 shows the diffraction pattern collected on these fibres. All diffraction peaks can be perfectly indexed to the crystalline NiO, not only in peak positions, but also in their relative intensity. The peaks can be indexed as (111), (220), (220), (311), (222), and (400) crystal plans of the crystalline cubic structure NiO, respectively. The NiO lattice constant calculated from the XRD data is  $a = 4.1765 \text{ \AA}$  which is in good agreement with that of the cubic NiO phase in standard JCPDS card.

The main physical and chemical parameter of NiO particles are shown in Table 1. It can be seen that the nickel oxide is fibrous with the characters of small grain diameter, low content of carbon, sulfur and ferrous.

**Table 1** Main physical and chemical parameters of nickel oxide powder

$w(\text{C})/\%$	$w(\text{Fe})/\%$	$w(\text{S})/\%$	BET specific surface/ ( $\text{m}^2 \cdot \text{g}^{-1}$ )
0.16	0.003	0.000 83	> 5.9

### 3.4 Growth mechanism of precursors and NiO fibres

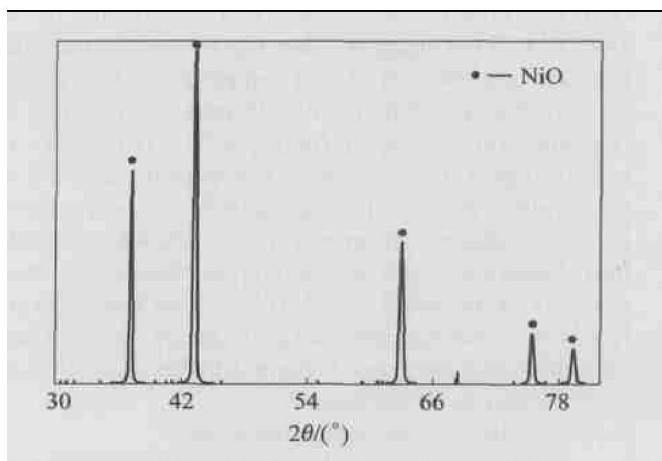


**Fig. 8** XRD pattern of fibrous NiO particles

At present, the growth mechanism of one-dimensional nanowires is one of the controversial subjects. Three growth mechanisms for crystalline fiber or whisker have been proposed: the vapor-liquid-solid (VLS) or solution-liquid-solid (SLS) growth mechanism<sup>[14,15]</sup>, template-induced methods<sup>[16]</sup> and oriented attachment mechanism<sup>[17,18]</sup>. The VLS and SLS growth mechanism requires flux particles that are molten under the reaction conditions or a catalyst whose boiling point is below the solvent, and are not suitable for the one-dimensional growth of NiO precursor fibres. For this work, oriented attachment is advised to explain the well-aligned growth of the precursor fibres. The proposed mechanism for the formation of precursor fiber can be expressed as follows: first,  $\text{NiCl}_2$  dissolves in water at certain temperature and  $(\text{NH}_4)_2\text{C}_2\text{O}_4$  gives  $\text{C}_2\text{O}_4^{2-}$  ions; secondly, a pri-



mary precursor nuclear forms in suitable supersaturation and begins to grow into precursor sheet; then the growing precursor sheets provide the initial template and induces the secondary nucleation and epitaxial growth of the second precursor sheet. This process continues in the same way and finally the fibrous precursors are obtained. In this mechanism, nanocrystals can join together with complete crystallographic alignment and eliminate free surfaces. The oriented attachment mechanism is strongly active only under conditions far from the isoelectric point. This point is confirmed by the experiment that the well-dispersed fibres precursor is obtained under  $\text{pH} = 8 - 10$  conditions. On the other hand, during the formation of precursor rods shape  $(\text{NH}_4)_2\text{C}_2\text{O}_4$  is thought to act as a template, resulting in the epitaxial growth of the precursor. NiO fibres are controlled by the in-situ growth mechanism, inherit the morphology of the precursor particles.

#### 4 CONCLUSIONS

1) The morphology of the precursor is a decisive element affecting the morphology of fibrous NiO particles obtained by thermal decomposition. Well dispersed and smaller size precursor powder is suitable for the preparation of the well dispersed fibrous NiO particles. Zeta potential value and surfactant PVP are important conditions for inhibition aggregation of nickelous complex precursors. The oriented attachment is proposed for the well-aligned growth of the NiO precursor fibres. The final product NiO inherits the morphology of the precursor.

2) In pyrolysis of the precursor, the operation parameters have obvious influences on the dispersion, particle size and specific surface area of the final NiO product, which include temperature and time for pyrolysis, the atmosphere, the pattern of temperature increase. When the pyrolysis is conducted under the conditions of temperature  $600 - 650^\circ\text{C}$  for  $30 - 60$  min and air flow  $0.1 - 0.124 \text{ dm}^3/\text{min}$ , the fibrous NiO may be produced with fine dispersion, large aspect ratio and  $5.944 \text{ m}^2/\text{g}$  of specific surface area.

#### REFERENCES

- [1] DUAN Xiang-feng, HUANG Yu, CUI Yi, et al. Indium phosphide nanowires as building blocks for nanoscale electronic and optoelectronic devices[J]. *Nature*, 2001, 409: 66 - 69.
- [2] LIU Sirmen, YUE Jun, Aharon G, et al. Synthesis of long silver nanowires from AgBr nanocrystals[J]. *Adv Mater*, 2001, 13(9): 656 - 658.
- [3] WANG Y Q, DUAN X F, CAO L M, et al. One dimensional growth mechanism of amorphous boron nanowires[J]. *Chem Phys Lett*, 2002, 359: 273 - 277.
- [4] Alfredo M M, Charles M L. A laser ablation method for the synthesis of crystalline semiconductor nanowires[J]. *Science*, 1998, 279: 208 - 211.
- [5] Hopwood J D, Mann S. Synthesis of barium sulfate nanoparticles and nanofilaments in reverse micelles and micromulsions[J]. *Chem Mater*, 1997, 9(8): 1819 - 1828.
- [6] PAN Zheng-wei, DAI Zhi-rong, WANG Zhong-lin. Nanobelts of semiconducting oxides[J]. *Science*, 2001, 291: 1947 - 1949.
- [7] XU Cong-kang, LIU Ying-kai, XU Guo-ding, et al. Preparation and characterization of CuO nanorods by thermal decomposition of  $\text{CuC}_2\text{O}_4$  precursor[J]. *Materials Research Bulletin*, 2002, 37: 2365 - 2372.
- [8] Setlur A A, Lauerhaas J M, Dai J Y, et al. A method for synthesizing large quantities of carbon nanotubes and encapsulated copper nanowires [J]. *Appl Phys Lett*, 1996, 69(3): 345 - 348.
- [9] YU Da-bin, WANG De-bao, MENG Zhan-yu, et al. Synthesis of closed PbS nanowires with regular geometric morphologies[J]. *J Mater Chem*, 2002, 12: 403 - 405.
- [10] ZHANG Y F, TANG Y H, WANG N, et al. One dimensional growth mechanism of crystalline silicon nanowires[J]. *Journal of Crystal Growth*, 1999, 197: 136 - 140.
- [11] Palchik O, Avivi S, Pinkert D, et al. Preparation and characterization of Ni/NiO composite using microwave irradiation and sonication[J]. *Nanostructure Materials*, 1999, 11(3): 415 - 420.
- [12] ZHANG Chuan-fu, ZHAN Jing, WU Jian-hui, et al. Preparation of fibrous nickel oxide particles[J]. *The Chinese Journal of Nonferrous Metals*, 2003, 13(6): 1440 - 1445.
- [13] Tadao S. Preparation of monodispersed colloidal particles[J]. *Advanced in Colloidal and Interface Science*, 1987, 28: 65 - 108.
- [14] Trentler T J, Hickman K M, et al. Solution-liquid-solid growth of crystalline III-V semiconductors: An analogy to vapor-liquid-solid growth[J]. *Science*, 1995, 270: 1791 - 1794.
- [15] Jayavel R, Mochiku T, Ooi S, et al. Vapour-liquid-solid (VLS) growth mechanism of superconducting Bi-Sr-Ca-Cu-O whiskers [J]. *Journal of Crystal Growth*, 2001, 229: 339 - 342.
- [16] HAN Wei-qiang, FAN Shou-shan, LI Qun-qing, et al. Synthesis of silicon nitride nanorods using carbon nanotube as a template[J]. *Appl Phys Lett*, 1997, 71(16): 2271 - 2273.
- [17] WANG De-bao, YU Da-bin, MO Ma-song, et al. Hydrothermal preparation of one-dimensional assemblies of PbS nanoparticles [J]. *Solid State Communication*, 2003, 125: 475 - 479.
- [18] Peng R L, Banfield J F. Morphology development and crystal growth in nanocrystalline aggregates under hydrothermal conditions: Insights from titania [J]. *Geochim Cosmochim Acta*, 1999, 63(10): 1549 - 1557.

(Edited by YUAN Sai-qian)